Article

Cell Reports

Potentiation of Synaptic GluN2B NMDAR Currents by Fyn Kinase Is Gated through BDNF-Mediated Disinhibition in Spinal Pain Processing

Graphical Abstract

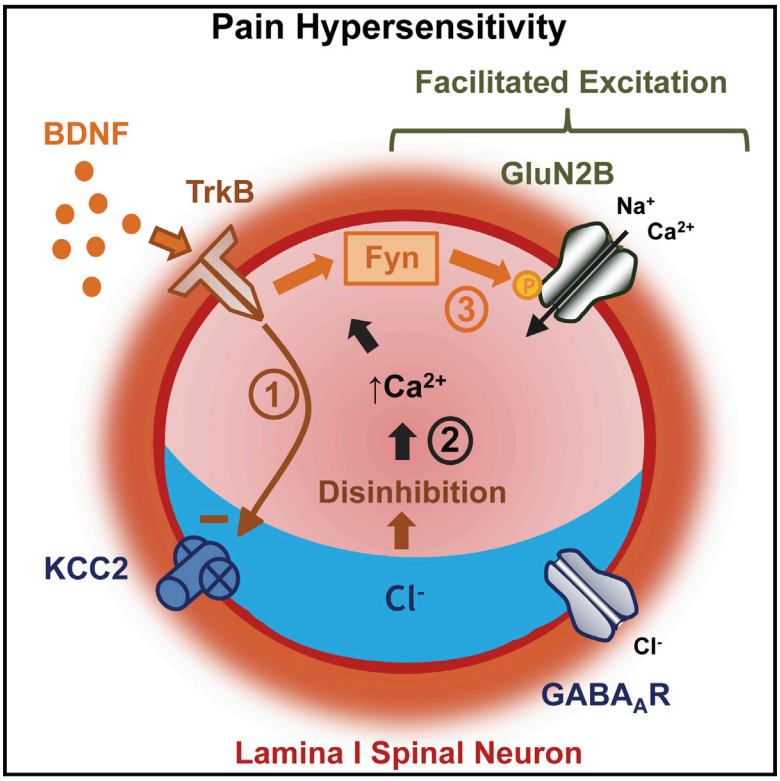

Highlights

- NMDAR currents at adult lamina I synapses are potentiated after nerve injury (PNI)
- BDNF mediates NMDAR potentiation through phosphorylation of GluN2B by Fyn
- Loss of Cl^--dependent inhibition is necessary for NMDAR potentiation by BDNF or PNI
- Blocking KCC2 or inducing Ca^{2+} entry permits synaptic NMDAR facilitation by BDNF

Authors

Michael E. Hildebrand, Jian Xu, Annemarie Dedek, ..., Simon Beggs, Paul J. Lombroso, Michael W. Salter

Correspondence

mike.hildebrand@carleton.ca (M.E.H.), mike.salter@utoronto.ca (M.W.S.)

In Brief

Lamina I spinal cord neurons are a hub for sensory integration and transmission within the pain processing network. Hildebrand et al. show that a BDNF-mediated loss of synaptic inhibition gates an increase in GluN2B-containing NMDAR responses at lamina I synapses in a peripheral nerve injury model of neuropathic pain.

Hildebrand et al., 2016, Cell Reports *17*, 2753–2765
December 6, 2016
http://dx.doi.org/10.1016/j.celrep.2016.11.024

Cell Reports
Article

Potentiation of Synaptic GluN2B NMDAR Currents by Fyn Kinase Is Gated through BDNF-Mediated Disinhibition in Spinal Pain Processing

Michael E. Hildebrand,[1,2,3,*] Jian Xu,[4] Annemarie Dedek,[3] Yi Li,[1,2] Ameet S. Sengar,[1] Simon Beggs,[1,2] Paul J. Lombroso,[4] and Michael W. Salter[1,2,5,*]
[1]Program in Neurosciences & Mental Health, Hospital for Sick Children, 686 Bay Street, Toronto, ON M5G 0A4, Canada
[2]Department of Physiology, University of Toronto, Toronto, ON M5S 1A1, Canada
[3]Department of Neuroscience, Carleton University, 1125 Colonel By Drive, Ottawa, ON K1S 5B6, Canada
[4]Child Study Center, Yale University School of Medicine, 230 South Frontage Road, New Haven, CT 06519, USA
[5]Lead Contact
*Correspondence: mike.hildebrand@carleton.ca (M.E.H.), mike.salter@utoronto.ca (M.W.S.)
http://dx.doi.org/10.1016/j.celrep.2016.11.024

SUMMARY

In chronic pain states, the neurotrophin brain-derived neurotrophic factor (BDNF) transforms the output of lamina I spinal neurons by decreasing synaptic inhibition. Pain hypersensitivity also depends on N-methyl-D-aspartate receptors (NMDARs) and Src-family kinases, but the locus of NMDAR dysregulation remains unknown. Here, we show that NMDAR-mediated currents at lamina I synapses are potentiated in a peripheral nerve injury model of neuropathic pain. We find that BDNF mediates NMDAR potentiation through activation of TrkB and phosphorylation of the GluN2B subunit by the Src-family kinase Fyn. Surprisingly, we find that Cl^--dependent disinhibition is necessary and sufficient to prime potentiation of synaptic NMDARs by BDNF. Thus, we propose that spinal pain amplification is mediated by a feedforward mechanism whereby loss of inhibition gates the increase in synaptic excitation within individual lamina I neurons. Given that neither disinhibition alone nor BDNF-TrkB signaling is sufficient to potentiate NMDARs, we have discovered a form of molecular coincidence detection in lamina I neurons.

INTRODUCTION

Pain hypersensitivity depends on maladaptive changes in neuronal activity within the peripheral, spinal, and brain nociceptive networks. The spinal nociceptive network in the dorsal horn is an interconnected matrix of inputs from primary afferents as well as from inhibitory and excitatory local circuit neurons and descending efferent fibers. Neurons in dorsal horn lamina I are an essential component of the spinal nociceptive network and are critical for acute as well as chronic pain signaling (Braz et al., 2014; Prescott et al., 2014).

The output of lamina I neurons is controlled by a delicate balance between synaptic excitation and inhibition and shifting the balance toward excitation leads to chronic pain (Woolf and Salter, 2000). This balance may be disrupted by reducing synaptic inhibition (disinhibition). A growing body of evidence has demonstrated that brain-derived neurotrophic factor (BDNF) is a major driver of disinhibition at lamina I synapses (Beggs and Salter, 2013; Ferrini and De Koninck, 2013). In the context of peripheral nerve injury (PNI), BDNF is released from activated microglia and binds to TrkB receptors on lamina I neurons (Beggs et al., 2012; Coull et al., 2005). Activated TrkB receptors downregulate the potassium-chloride co-transporter, KCC2, resulting in increased intracellular Cl^-, attenuated GABAergic inhibition, and increased action potential firing in lamina I neurons (Coull et al., 2003, 2005; Keller et al., 2007).

Pain-producing changes in the balance between excitation and inhibition may also be mediated by enhancing excitation within the spinal nociceptive network. Excitation is driven by glutamatergic synaptic transmission, and the N-methyl-D-aspartate receptor (NMDAR) class of glutamate receptors is prominently implicated in spinal mechanisms of chronic pain (Bourinet et al., 2014). Blocking NMDAR activity of receptors containing the GluN2B subunit using pharmacological or genetic approaches blocks pain hypersensitivity in animal models of chronic pain. Moreover, behavioral and biochemical studies show that enhancement of NMDAR function by Src family kinases is critical for pain hypersensitivity (Abe et al., 2005; Liu et al., 2008).

A major open question is where is the critical locus of change in glutamate receptor function within the highly interconnected matrix that is the spinal nociceptive network. Here, we tested the hypothesis that in pain hypersensitivity, there is enhanced glutamatergic synaptic transmission onto neurons in lamina I. In order to properly characterize the postsynaptic responses at lamina I glutamatergic synapses, it was necessary to avoid activating the nociceptive network, which includes prolonged polysynaptic excitatory responses that contaminate direct excitatory synaptic responses (Todd, 2010). Thus, we studied miniature excitatory postsynaptic currents (mEPSCs) in lamina I neurons, as these mEPSCs are direct synaptic responses (Hildebrand

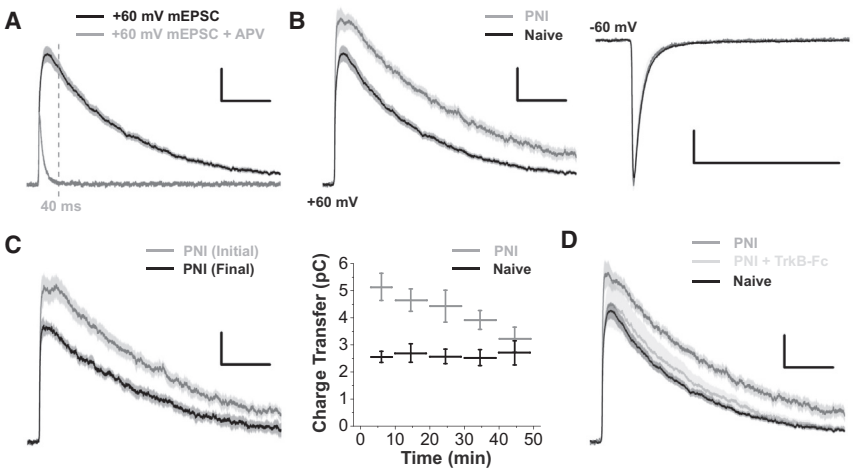

Figure 1. NMDAR mEPSCs in Lamina I Neurons Are Reversibly Potentiated by BDNF in the PNI Model of Neuropathic Pain

(A) Average outward mEPSC traces at +60 mV from lamina I neurons in spinal slices of naive rats in the absence (black, n = 20) and presence (gray, n = 3) of 100 μM APV.

(B) Left: average mEPSC traces at + 60 mV in rats with PNI (gray, n = 9) compared to naive rats (black, n = 20). Right: average mEPSC traces at −60 mV in rats with PNI (gray, n = 5) compared to naive rats (black, n = 13).

(C) Left: averaged mEPSC traces from rats with PNI during an initial recording period (gray) and during a final period (30–50 min) of recording (black, n = 7). Right: time course of NMDAR charge transfer (averaged every 10 min, n = 4 each).

(D) Average mEPSC traces from naive rats (black) and rats with PNI (gray) as well as from rats with PNI that had slices treated with 200 ng/mL TrkB-F_c before recording (light gray, n = 9). Current traces are represented as means (dark lines) ± SEM (lighter bars) of mEPSCs from all averaged cells. Scale bars, 100 ms (x axes); 5 pA (y axes).

et al., 2014). We found that NMDAR-mediated mEPSCs were enhanced in a PNI model of chronic pain. Because the enhancement was mediated by BDNF-TrkB signaling, we tested whether there is functional crosstalk between potentiation of NMDAR-mediated excitation and loss of GABAergic inhibition. We found that BDNF-mediated disinhibition led to enhancement of GluN2B NMDAR responses via Fyn activation in naive animals and, conversely, blocking disinhibition reversed the enhancement after PNI. Thus, our findings show that enhanced excitation of lamina I neurons is gated by disinhibition.

RESULTS

The NMDAR but Not the AMPAR Component of mEPSCs in Lamina I Neurons Is Increased following Peripheral Nerve Injury

To investigate synaptic glutamatergic responses in lamina I neurons, we made whole-cell patch clamp recordings on visualized neurons in lamina I in acute spinal slices from adult rats. When we recorded at a holding potential of −60 mV, we observed spontaneously occurring, rapidly rising, and decaying inward currents that were eliminated by the AMPAR antagonist CNQX, demonstrating that these were mEPSCs. Holding the membrane potential at +60 mV revealed a slowly decaying NMDAR component of the mEPSCs that was blocked by 100 μM APV (Figure 1A). Thus, the currents we recorded here corresponded to bi-component, AMPAR/NMDAR mEPSCs described previously (Hildebrand et al., 2014). To clearly separate the NMDAR-mediated component from the AMPAR-mediated component during recordings at +60 mV, we calculated the NMDAR component as that beginning 40 ms after the onset of the mEPSC and extending to 500 ms after mEPSC onset (Table S1). AMPAR currents were studied at a holding potential of −60 mV.

To determine whether these glutamatergic synaptic responses of lamina I neurons are affected during pathological pain processing, we studied mEPSCs in neurons from rats that had received a PNI (Mosconi and Kruger, 1996; Pitcher et al., 1999). PNI is widely used as a model of peripheral neuropathic pain and pain hypersensitivity is inferred by a lowering of the mechanical paw withdrawal threshold ipsilateral to the nerve injury. We included only animals in which the paw withdrawal threshold was significantly reduced compared to the same paw before PNI (n = 23 animals). The recordings were made from slices taken from animals 10–17 days after PNI, when the mechanical hypersensitivity has reached maximum. We found that the frequency of mEPSCs was not affected by PNI (PNI: 4.5 ± 1.8 Hz, n = 5; naive 3.6 ± 0.9, n = 13, p = 0.61). Moreover, we found that the AMPAR mEPSCs in lamina I neurons were not altered in neurons from animals with PNI (Figure 1B): peak (−23.6 ± 1.2 pA), rise time (0.9 ± 0.2 ms), and decay time constant (5.9 ± 0.9 ms) of the AMPAR mEPSCs after PNI (n = 5 neurons) were not significantly different than those from naive rats (−22.0 ± 1.2 pA, p = 0.45; 1.2 ± 0.1 ms, p = 0.27; 6.7 ± 0.5 ms, p = 0.43, respectively; n = 13 neurons). By contrast, we found that the NMDAR component of the mEPSCs was significantly increased after PNI (Figure 1B). We used charge transfer as a robust measure of the NMDAR component of the mEPSCs (Hildebrand et al., 2014) and observed that the charge transfer in neurons from rats with PNI (5.27 ± 0.35 pC, n = 9 neurons) was greater than that in naive rats (3.20 ± 0.22 pC, n = 20 neurons; p = 0.000021). The NMDAR component of the mEPSCs in sham-operated rats (2.75 ± 0.52 pC, n = 6) was not different from that in naive rats (p = 0.37). From these findings, we conclude that the NMDAR component, but not the AMPAR component, of mEPSCs in lamina I neurons was significantly potentiated following PNI.

BDNF-TrkB Signaling Mediates the Potentiation of NMDAR mEPSCs by PNI

Strikingly, we observed a progressive decrease in the NMDAR component of mEPSCs during recordings of lamina I neurons from rats with PNI but not during recordings in neurons from naive rats (Figure 1C; Table S2). By comparison, the AMPAR component of the mEPSCs was stable during recording from

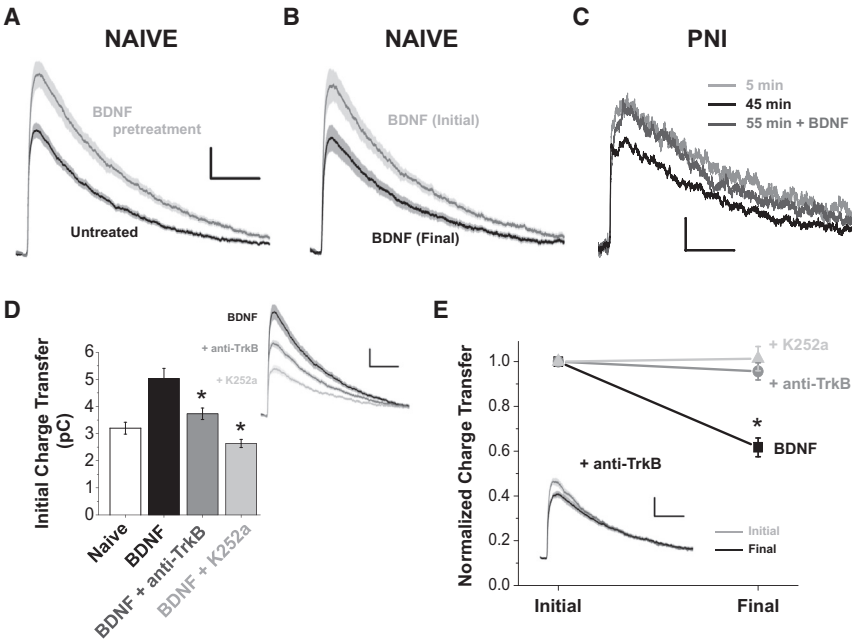

Figure 2. BDNF Is Sufficient to Facilitate NMDAR mEPSCs

(A) Average initial mEPSC traces in slices of naive rats treated with (gray, n = 14) or without (black, n = 20) 50 ng/mL BDNF.

(B) Average mEPSC traces from BDNF-treated slices during initial (gray) and final (black, 20 to 50 min) periods of recording (n = 10).

(C) mEPSC traces from a rat with PNI during an initial recording period (gray), a later recording period (black), and subsequent perfusion of 100 ng/mL recombinant BDNF protein for 5–15 min (dark gray).

(D) Average initial mEPSC traces (top) and associated NMDAR charge transfer values (bottom) from spinal slices of naive rats pre-treated with BDNF alone (black, n = 14), BDNF and 2 mg/mL anti-TrkB (gray, n = 7), or BDNF followed by intracellular 100 nM K252a during recording (light gray, n = 8). *p < 0.05 compared to BDNF pre-treatment alone.

(E) Plot of final charge transfer values normalized to initial values. *p < 0.05 compared to initial charge transfer values for given treatment. *Inset*, average mEPSC traces at +60 mV during initial (gray) and final (black) recording periods for slices pre-treated with BDNF and anti-TrkB (n = 5). Scale bars, 100 ms (x axes); 5 pA (y axes).

All current traces and plots are represented as means ± SEM.

either PNI or naive rats (not illustrated). In neurons from rats with PNI, the NMDAR charge transfer decreased from an initial value of 5.17 ± 0.47 pC to 3.08 ± 0.37 pC (n = 7 neurons, p = 0.000030) after 30 min of recording. The NMDAR charge transfer at the end of the recordings from these neurons was not different from the charge transfer in neurons from naive rats (p = 0.47; Figure 1C). These findings indicate that the potentiation of the NMDAR component of the mEPSCs in neurons from rats with PNI was gradually lost during the recordings and that the NMDAR mEPSCs returned to the basal level observed in neurons from naive animals.

The neurons were continuously superfused with extracellular recording solution during the recording period, and we questioned whether the decrease in NMDAR mEPSCs in neurons from rats with PNI was due to progressive loss of an endogenous, extracellular potentiating substance. Given the key role of BDNF in pain hypersensitivity (Beggs and Salter, 2013; Ferrini and De Koninck, 2013), we considered the possibility that BDNF might be such a potentiating substance. To test this possibility, we treated spinal cord slices from rats with PNI with a BDNF-sequestering fusion protein, TrkB-Fc (Ninkina et al., 1997), beginning at least 10 min prior to recording and continuing throughout the recording period. In contrast to the recordings without TrkB-Fc treatment, we found that the NMDAR charge transfer was stable during recordings (n = 6, p = 0.30) in neurons from PNI rats treated with TrkB-Fc (200 ng/mL). Moreover, the initial NMDAR charge transfer in neurons from PNI rats treated with TrkB-Fc was significantly less than that in PNI neurons not treated with TrkB-Fc (n = 9, p = 0.014, Figure 1D). In addition, the NMDAR charge transfer in PNI neurons treated with TrkB-Fc was not different from the final NMDAR charge transfer in neurons from PNI rats (n = 9 and 7 neurons, respectively, p = 0.62) nor from that in neurons from naive rats (n = 20 neurons, p = 0.62). Together, these findings indicate that prior to the beginning of the recordings in neurons from PNI animals, the pre-treatment with TrkB-Fc occluded the decline in NMDAR mEPSCs. The observation that the NMDAR charge transfer in neurons from PNI rats remained constant or increased during the first 10 min of recording suggests that the decline in NMDAR responses was not due to loss of an intracellular signal through dialysis of the patch pipette solution. Therefore, we conclude that the potentiation of NMDAR mEPSCs in lamina I neurons following PNI depends upon endogenously released BDNF.

To test whether BDNF is sufficient to cause potentiation of NMDAR mEPSCs, we pre-treated spinal slices from naive animals with recombinant BDNF (50 ng/mL BDNF, 75 ± 3 min, n = 14 neurons). We found that the initial NMDAR charge transfer in BDNF-pre-treated slices (5.03 ± 0.37 pC; n = 14 neurons) was significantly larger than that in neurons from untreated slices (3.20 ± 0.22 pC; n = 20 neurons; p = 0.000088; Figures 2A). During these experiments, we stopped the BDNF treatment just prior to recording and observed a progressive decrease in the NMDAR mEPSCs (Figure 2B) comparable to the decline in the NMDAR component during recordings in neurons from PNI rats (cf. Figure 1C). To determine whether we could reverse the loss of NMDAR mEPSC charge transfer during recordings from PNI animals, we applied BDNF after the currents had declined (Figure 2C; Table S3). NMDAR currents significantly increased by 55% ± 14% (n = 5 neurons, p = 0.0086) following BDNF administration (100 ng/mL, 7–20 min), indicating that the decline in NMDAR mEPSCs was rescued by exogenous BDNF. The finding that NMDAR responses were potentiated by exogenous BDNF at this later time point further supports the conclusion that the initial decline in NMDARs was not due to whole-cell dialysis. Together,

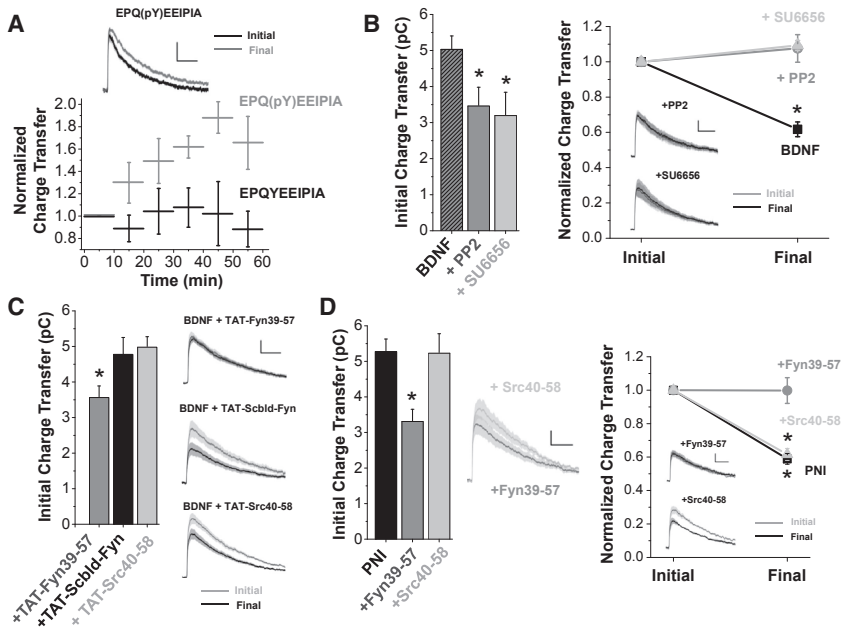

Figure 3. The Potentiation of NMDAR mEPSCs by BDNF/ PNI Requires Fyn but Not Src

(A) Time course of NMDAR charge transfer with either 1 mM EPQ(pY)EEIPIA (gray, n = 4) or 1 mM EPQYEEIPIA (black, n = 3) in the intracellular pipette solution. *Inset*, average mEPSC traces during initial (black) and final (gray, 40+ min) recording periods, with 1 mM EPQ(pY)EEIPIA in the intracellular solution.

(B) Left: plot of initial NMDAR charge transfer for slices pre-treated with BDNF (shaded, cf. Figure 3A), BDNF and 1 μM PP2 (gray, n = 6), or BDNF and 10 μM SU6656 (light gray, n = 5). *p < 0.05 compared to BDNF pre-treatment alone. Right: plot of normalized charge transfer values for the same pre-treatment conditions as left, with inset average mEPSC traces for pre-treatment with BDNF and PP2 (top) or BDNF and SU6656 (bottom). *p < 0.05 compared to initial charge transfer value for given treatment.

(C) Left: plot of initial NMDAR charge transfer for slices pre-treated with BDNF and 10 μM TAT-Fyn39-57 (gray, n = 9), BDNF and 10 μM TAT-Scbld-Fyn (black, n = 7), or BDNF and 10 μM TAT-Src40-58 (light gray, n = 9). *p < 0.05 compared to BDNF pre-treatment alone. Right: average mEPSC traces during initial (gray) and final (black) recording periods for the pre-treatment conditions to the left.

(D) Left: plot of initial NMDAR charge transfer from PNI rats during control recordings (black, n = 9) or recordings with intracellular dialysis of Fyn39-57 (gray, n = 6) or Src40-58 (light gray, n = 7). Middle: average initial mEPSCs of PNI rats with intracellular Src40-58 (light gray) or intracellular Fyn39-57 (gray). Right: plot of normalized charge transfer values during initial and final recording periods for the same treatment conditions in PNI rats as left, with inset average mEPSC traces. Scale bars, 100 ms (x axes); 5 pA (y axes).

All current traces and plots are represented as means ± SEM.

these findings indicate that BDNF is not only necessary for the potentiation following PNI but is also sufficient to induce a potentiation of synaptic NMDAR currents in lamina I neurons.

To determine whether the potentiation of NMDAR mEPSCs by BDNF is mediated through activation of its cognate receptor, TrkB, we utilized a function-blocking anti-TrkB antibody (anti-TrkB) (Coull et al., 2005; Prescott et al., 2014). In spinal slices from naive rats, co-treatment of anti-TrkB (2 μg/mL) with BDNF (n = 7 neurons) prevented the potentiation of NMDAR mEPSCs (Figure 2D) and the subsequent decline in NMDAR mEPSCs (Figure 2E) seen in neurons pre-treated with BDNF but not anti-TrkB (cf. Figure 2A). To test whether TrkB was activated directly in the neuron in which NMDAR mEPSCs were potentiated, we intracellularly administered the TrkB inhibitor, K252a (Tapley et al., 1992), into the recorded neuron through the patch pipette. Because we administered K252a directly into the cell, we used near IC_{50} concentrations (100 nM) to minimize inhibition of TrkB in neighboring neurons. In neurons with intracellularly administered K252a (n = 8 neurons), we observed neither the BDNF-induced increase in NMDAR charge transfer (Figure 2D) nor the subsequent decline in NMDAR mEPSCs during recordings (Figure 2E). Therefore, we conclude that the potentiation by BDNF of synaptic NMDAR responses in a given lamina I neuron is mediated by activating TrkB on that neuron.

Potentiation of NMDAR mEPSCs by BDNF Requires Fyn Kinase Activity

As upregulation of NMDARs by Src family protein tyrosine kinases (Wang and Salter, 1994) is implicated in models of pain hypersensitivity (Bourinet et al., 2014), we investigated whether Src family kinases (SFKs) participate in the BDNF-mediated potentiation of NMDAR mEPSCs in lamina I neurons. First, we found that the phosphopeptide SFK activator EPQ(pY)EEIPIA (1 mM, n = 4 neurons, p = 0.0056), but not the inactive EPQYEEIPIA (1 mM, n = 3 neurons, p = 0.47), caused a progressive increase in NMDAR charge transfer when administered intracellularly through the patch pipette (Figure 3A). Thus, in lamina I neurons synaptic NMDAR currents can be upregulated by activating SFKs.

Next, we tested for SFK involvement in BDNF-mediated potentiation of NMDAR mEPSCs. We found that the BDNF-induced increase in NMDAR charge transfer was prevented (Figure 3B, left) by pre-administering the SFK inhibitor PP2 (1 μM; n = 6 neurons). Pre-treating with PP2 also precluded the in-recording decline in NMDAR charge transfer normally observed in neurons pre-treated with BDNF without PP2 (Figure 3B, right). Administering PP2 acutely to spinal slices from naive animals had no effect on NMDAR charge transfer (n = 4 neurons, p = 0.46; Figure S1), implying that PP2 does not directly inhibit NMDARs. Also, the lack of effect of PP2 on NMDAR mEPSCs indicates that in lamina I neurons under basal conditions there is no ongoing upregulation of NMDAR mEPSCs by SFKs. The effects of PP2 on BDNF potentiation of NMDARs were mimicked by a structurally distinct SFK inhibitor, SU6656 (10 μM; n = 5 neurons; Figure 3B). Thus, we conclude that SFK activity is necessary for the BDNF-mediated potentiation of NMDAR mEPSCs in lamina I neurons.

Because two individual SFK members, Src and Fyn, are implicated in chronic pain hypersensitivity (Abe et al., 2005; Liu et al.,

2008), we tested whether Src or Fyn is required for the potentiation of NMDAR mEPSCs by BDNF. We utilized membrane-permeable TAT-fusion peptide inhibitors that differentially block the upregulation of NMDAR currents by Src kinase itself, TAT-Src40-58 (Liu et al., 2008), or by Fyn kinase, TAT-Fyn39-57 (Yang et al., 2012). We examined the effects of the TAT peptides (10 μM) on the BDNF-induced potentiation in lamina I neurons from naive rats. Pre-treating with TAT-Fyn39-57 together with BDNF (n = 9 neurons) prevented the potentiation of NMDAR mEPSCs (Figure 3C) and the subsequent decline in NMDAR mEPSCs (Figure 3C) observed in neurons pre-treated with BDNF alone. However, pre-treatment with a TAT-fusion peptide in which the Fyn39-57 sequence was scrambled (TAT-Scbld-Fyn, n = 7 neurons) did not prevent the BDNF potentiation: the NMDAR charge transfer in neurons treated with TAT-Scbld-Fyn was not different from that in neurons treated with BDNF alone and the characteristic in-recording decline in the NMDAR mEPSCs was observed (Figure 3C). In contrast to TAT-Fyn39-57, TAT-Src40-58 (n = 9 neurons) did not prevent the BDNF-induced increase in NMDAR charge transfer nor the subsequent in-recording decline in the NMDAR mEPSCs (Figure 3C).

As these findings indicate that the potentiation of NMDAR mEPSCs by BDNF depends upon Fyn kinase but not Src kinase, we tested whether Fyn, but not Src, is required for the potentiation of NMDAR mEPSCs following PNI. In these experiments, we utilized membrane-impermeant versions of the peptides—Fyn39-57 and Src40-58 (30 μg/mL)—which were administered directly into the neurons during recordings to allow us to determine whether Fyn, or Src, was required in the neuron under study. We found in recordings from PNI animals that the NMDAR charge transfer in neurons in which Fyn39-57 was administered intracellularly (n = 6 neurons) was significantly less than that in neurons without Fyn39-57 (Figure 3D, left). In addition, there was no in-recording decline in NMDAR mEPSCs in neurons recorded with Fyn39-57 (Figure 3D, right). Moreover, after PNI the NMDAR charge transfer in neurons recorded with Fyn39-57 was not different from that in neurons from naive rats not receiving Fyn39-57 (PNI + Fyn 3.31 ± 0.34 pC, n = 6 neurons; naive 3.20 ± 0.22 pC, n = 20 neurons, p = 0.81). The effects of Fyn39-57 on NMDAR charge transfer in neurons from PNI rats were not produced by intracellularly administering Src40-58 (n = 7 neurons): NMDAR charge transfer and subsequent in-recording decline were not different from those in neurons without peptide administration (Figure 3D).

BDNF Activates Fyn but Not Src to Drive the Phosphorylation and Potentiation of GluN2B NMDARs

Because Fyn was required for the potentiation of synaptic NMDARs by either BDNF or nerve injury, we next tested whether activation of Fyn was sufficient to potentiate NMDARs at adult lamina I synapses. We found that activation of intracellular SFKs with EPQ(pY)EEIPIA significantly ($p < 0.05$) increased NMDAR mEPSCs when Src was blocked with intracellular Src40-58 (n = 5) but not when Fyn was blocked with intracellular Fyn39-57 (n = 6) (Figure 4A). We previously found that SFKs are differentially coupled to specific NMDAR GluN2 subunits, with Src potentiating GluN2A-containing receptors and Fyn potentiating GluN2B-containing receptors (Yang et al., 2012). Here, we found that the component of NMDAR mEPSCs that was potentiated by BDNF had a decay time constant of 276 ms, which is consistent with NMDARs containing GluN1 together with GluN2B (Figure 4B). We therefore tested whether GluN2A and/or GluN2B is required for the potentiation of NMDAR mEPSCs by BDNF. In slices treated with BDNF and a GluN2A selective antagonist, TCN-201 (3 μM), the initial NMDAR charge transfer (4.24 ± 0.22 pC; n = 8) was significantly greater than slices treated with the GluN2A antagonist alone (2.86 ± 0.25 pC; n = 12; p = 0.0012), with the same decline in NMDAR mEPSCs observed for BDNF pre-treatment alone (Figure 4C). In contrast, treating slices with BDNF and a GluN2B selective antagonist, Ro25-6981 (1 μM), prevented the potentiation and subsequent decline of NMDAR mEPSCs (Figure 4C): the initial NMDAR charge transfer was not significantly different for BDNF and Ro25-6981 (1.54 ± 0.22 pC; n = 6) compared to treatment with Ro25-6981 alone (1.23 ± 0.17 pC; n = 12; p = 0.30).

Next, we used biochemical approaches to investigate whether BDNF treatment altered Fyn-meditated phosphorylation and synaptic localization of NMDAR subunits in the superficial dorsal horn (SDH). We first immunoprecipitated Fyn or Src from the synaptosomal fraction of SDH tissue, followed by detection with phospho-SFK antibodies. Phosphorylation of two tyrosine residues regulate the activity of these kinases, with phosphorylation of Tyr^{420} activating Fyn (Tyr^{416} in Src) and phosphorylation of Tyr^{531} inhibiting Fyn (Tyr^{527} in Src) (Ingley, 2008; Salter and Kalia, 2004). Treatment of SDH tissue with BDNF led to a significant increase in Fyn phosphorylation at Tyr^{420} (p = 0.012) and a concomitant decrease at Tyr^{531} (p = 0.014), indicating increased activation of Fyn at SDH synapses (n = 6 slices, Figure 5A). In contrast, we found no changes in Src phosphorylation at either Tyr^{416} (p = 0.58) or Tyr^{527} (p = 0.48) (n = 6, Figure 5A) as well as no change in total Src or Fyn protein levels (Figure 5B, data not shown).

We also tested the phospho-SFK antibody without immunoprecipitation and found a significant increase in SFK phosphorylation at this Tyr residue (Tyr^{420}/Tyr^{416}, Figure 5B, top; Data S1). As phosphorylation of Src was not altered by BDNF (Figure 5A), we conclude that this likely reflects an increase in Fyn phosphorylation at Tyr^{420}. Activated Fyn potentiates GluN2B-containing NMDARs by phosphorylating Tyr^{1472} on the GluN2B subunit (Salter and Kalia, 2004). Consistent with our findings of a Fyn-dependent potentiation of GluN2B-mediated synaptic responses, we found increased phosphorylation of GluN2B at Tyr^{1472} upon BDNF treatment (p = 0.023) as well as increased localization of GluN2B protein in SDH synaptosomes (p = 0.012) (n = 8 slices, Figure 5B, middle). In contrast, we found that BDNF treatment did not alter the phosphorylation of GluN2A at an analogous residue (Tyr^{1325}) (p = 0.84) nor total GluN2A levels (p = 0.59) (n = 8 slices, Figure 5B, bottom). Moreover, BDNF treatment had no effect on Fyn or GluN2B phosphorylation or expression in synaptosomes from deep dorsal horn and ventral horn tissue (Figure S2A) nor in SDH total homogenates (Figure S2B).

To test whether Fyn kinase was required for the BDNF-mediated increase in GluN2B phosphorylation and synaptic localization, we treated SDH tissue with BDNF and TAT-Fyn39-57. We found that co-administration of TAT-Fyn39-57 abolished the increase in phosphorylation of GluN2B at Tyr^{1472} (p = 0.99) and

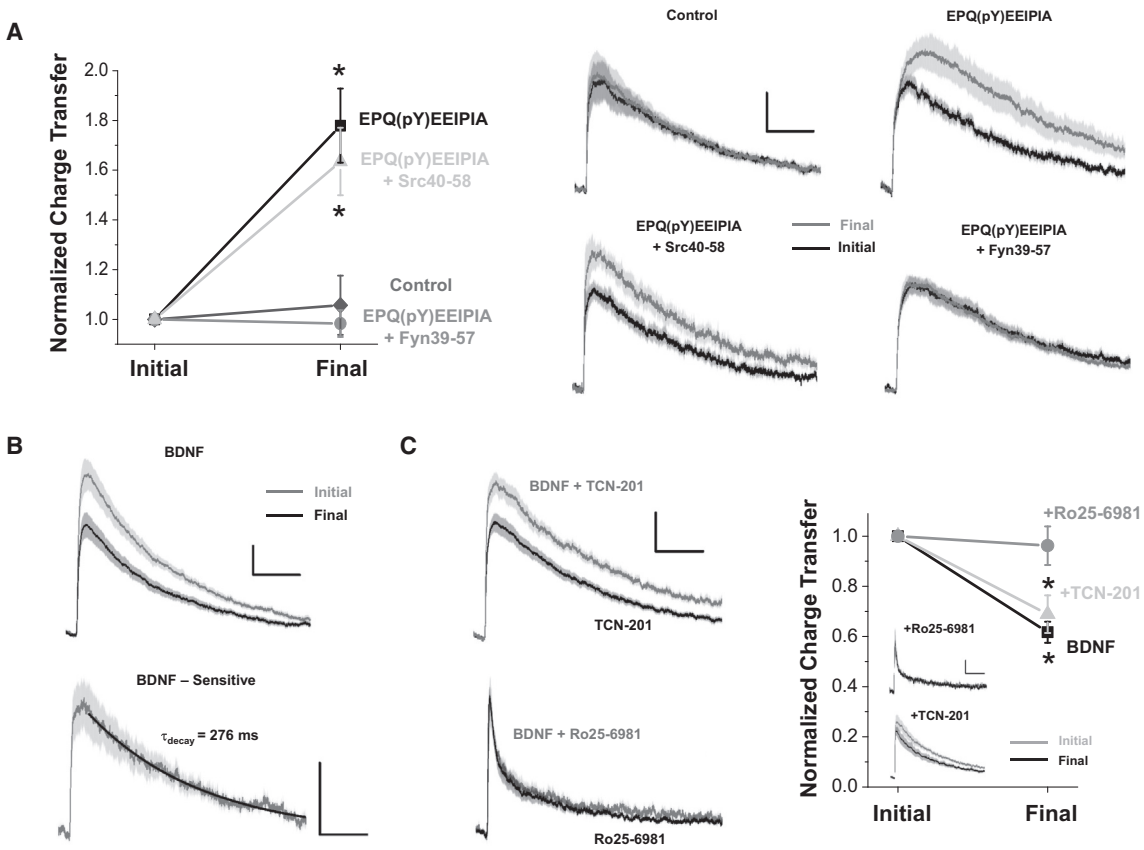

Figure 4. Fyn but Not Src Directly Mediates the Potentiation of GluN2B-Containing NMDAR Responses at Lamina I Synapses

(A) Plot of initial versus final NMDAR charge transfer values (left) and averaged traces (right) for recordings on naive lamina I neurons with control internal solution (n = 5), EPQ(pY)EEIPIA (n = 6), EPQ(pY)EEIPIA + Src40-58 (n = 5), or EPQ(pY)EEIPIA + Fyn39-57 (n = 6) in the patch pipette.

(B) Subtraction of final mEPSCs from initial mEPSCs in BDNF pre-treated slices yields a BDNF-sensitive mEPSC component (n = 10).

(C) Left: average initial mEPSC traces from slices pre-treated with TCN-201 (n = 12) versus BDNF and TCN-201 (n = 8) (top) or Ro25-6981 (n = 12) versus BDNF and Ro25-6981 (n = 6) (bottom). Right: plot of normalized charge transfer values during initial and final recording periods for slices pre-treated with BDNF (n = 10), BDNF and Ro25-6981 (n = 4), or BDNF and TCN-201 (n = 6), with inset average mEPSC traces. *p < 0.05 compared to initial charge transfer value for given treatment. Scale bars, 100 ms (x axes); 5 pA (y axes).

All current traces and plots are represented as means ± SEM.

the increase in total synaptosomal GluN2B (p = 0.93) observed for BDNF alone (n = 8 slices, Figure 5B, middle). In slices treated with TAT-Scbld-Fyn and BDNF, we found an increase in phosphorylated GluN2B (p = 0.049) and total GluN2B (p = 0.28) compared to control-treated slices, albeit below the significance threshold for the latter (n = 8 slices). Importantly, the increase in phosphorylation of Fyn at Tyr^{420} was preserved when slices were treated with BDNF and TAT-Fyn39-57 (n = 8 slices, p = 0.025; Figure 5B, top), showing that TAT-Fyn39-57 blocks Fyn-GluN2B interactions rather than the regulation of Fyn activity itself. These findings together suggest that synaptic NMDAR currents in lamina I neurons are potentiated following PNI by BDNF-induced stimulation of TrkB, activation of Fyn kinase, and subsequent phosphorylation of GluN2B-containing NMDARs.

BDNF-Mediated Disinhibition Is Required for the Potentiation of GluN2B NMDARs by Fyn after PNI

BDNF is a well-known mediator of PNI-induced pain hypersensitivity via TrkB-mediated blockade of KCC2 and subsequent suppression of $GABA_A$- and glycine-mediated inhibition of neurons in spinal lamina I (Beggs and Salter, 2013; Ferrini and De Koninck, 2013). Hence, we wondered whether this type of disinhibition may be required for the potentiation of NMDAR mEPSCs in lamina I neurons. As $GABA_A$ and glycine receptors are permeable to HCO_3^-, in addition to Cl^-, disinhibition driven by blockade of KCC2 is dependent upon HCO_3^- efflux (Price et al., 2009; Staley et al., 1995) and can be reversed by lowering intracellular HCO_3^- via inhibiting carbonic anhydrase (Kaila et al., 2014). Therefore, we examined the potential involvement of disinhibition in the BDNF-mediated potentiation of NMDAR currents by using the membrane-permeant inhibitor of carbonic anhydrase, acetazolamide. Acetazolamide has been found to reverse depolarizing shifts in $GABA_A$-receptor currents in lamina I neurons (Ferrini et al., 2013).

Pre-treating slices from naive rats with acetazolamide (10 μM) together with BDNF prevented the potentiation of NMDAR mEPSCs induced by BDNF pre-treatment alone (Figure 6A, left). Specifically, the NMDAR charge transfer in neurons pre-treated

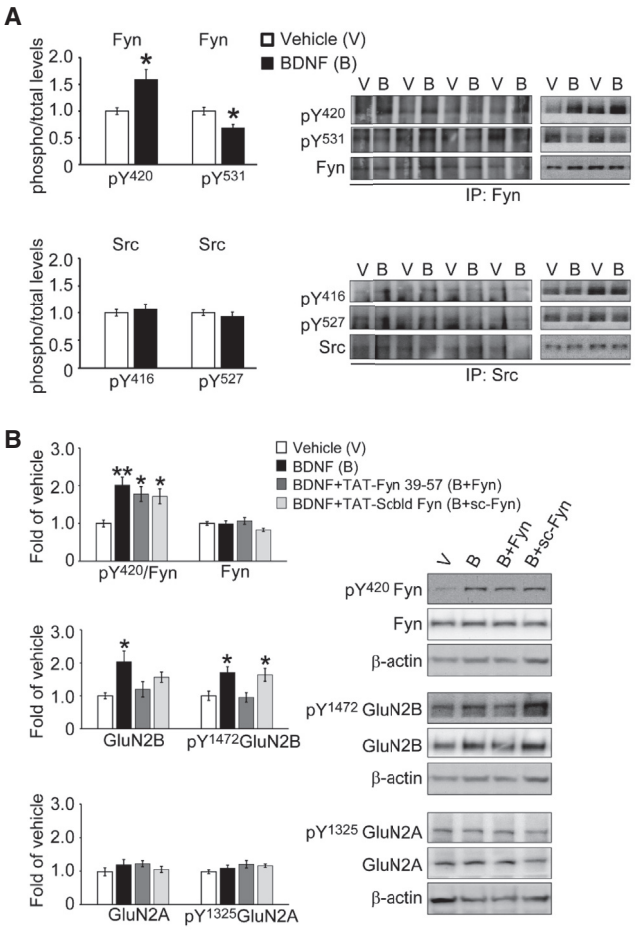

Figure 5. BDNF Activates Fyn but Not Src to Drive Trafficking and Phosphorylation of GluN2B NMDARs Selectively at Superficial Dorsal Horn Synapses

(A) Fyn or Src were immunoprecipitated from synaptic fractions of SDH. Western blots using phospho-specific antibodies (right), with phosphorylation levels normalized to total protein levels (left). *p < 0.05, n = 6.

(B) Western blots from synaptic fractions of SDH treated with either saline, BDNF, BDNF and TAT-Fyn39-57, or BDNF and TAT-Scbld-Fyn for 70 min. Blots (n = 8, right) were probed with the antibodies indicated. Phospho-Fyn was normalized to Fyn and then to beta-actin as a loading control while all other targets were normalized to beta-actin directly (left). *p < 0.05 using one-way ANOVA with Tukey's post hoc test.

All plots are represented as means ± SEM.

with BDNF and acetazolamide (3.24 ± 0.34 pC, n = 8 neurons) was significantly less than that in neurons treated with BDNF alone (p = 0.0045) and was not significantly different from that in untreated neurons from naive rats (3.20 ± 0.22 pC, n = 20 neurons, p = 0.92). Also, the in-recording decline of NMDAR mEPSCs, characteristic of neurons pre-treated with BDNF alone was not seen in neurons pre-treated with BDNF together with acetazolamide (Figure 6A, right). We found that pre-treating slices from naive rats with acetazolamide alone had no significant effect on NMDAR mEPSCs, suggesting that disinhibition does not regulate NMDAR currents under basal conditions (Figure 6B). However, in recordings from rats with PNI, treating slices with acetazolamide prior to recording significantly reduced the amplitude of the initial NMDAR mEPSCs to 3.94 ± 0.46 pC (n = 7 neurons; p = 0.035 compared to PNI alone)—a level not different from that of the charge transfer in neurons from rats without PNI (Figure 6C, left, p = 0.88). Acetazolamide pre-treatment also prevented the in-recording decline of NMDAR mEPSCs in rats with PNI (Figure 6C, right). It is conceivable that the effects of acetazolamide might have been due to blockade of BDNF activation of TrkB receptors. However, we found that acetazolamide (10 μM) did not affect activation of TrkB by BDNF (Figure S3) and thus acetazolamide was not acting to prevent BDNF from activating TrkB.

In contrast to SDH tissue treated with BDNF alone, treatment of slices with BDNF and acetazolamide prevented the BDNF-dependent increase in phosphorylation of Fyn at Tyr^{420} (p = 0.97) as well as the increase in phosphorylated GluN2B (pY^{1472}, p = 0.99) and total GluN2B (p = 0.99) in SDH synaptosomes (n = 8 slices, Figure 6D; Data S1). Moreover, treatment of slices with acetazolamide alone had no effect on Fyn phosphorylation at Tyr^{420} (p = 0.94), GluN2B phosphorylation at Tyr^{1472} (p = 0.99), or total synaptic GluN2B levels (p = 0.99, n = 8 slices, Figure 6D), suggesting there is no basal level of disinhibition within the naive SDH. Similarly, treatment with either acetazolamide or acetazolamide and BDNF had no effect on levels of pY^{420} Fyn, pY^{1472} GluN2B, or GluN2B at deep dorsal horn and ventral horn synapses (Figure S4). Thus, we conclude that BDNF-induced disinhibition is necessary for the Fyn-mediated potentiation of GluN2B-containing NMDARs produced by exogenous BDNF or by PNI.

KCC2 Downregulation Primes Lamina I Neurons for NMDAR Potentiation by BDNF

To test whether the disinhibition mediated by suppressing KCC2 is sufficient to potentiate synaptic NMDAR responses, we used the pharmacological inhibitor of KCC2, VU0240551 (Delpire et al., 2009). We applied VU0240551 to spinal slices from naive rats at a concentration (50 μM) known to increase intracellular [Cl^-] and decrease GABA-mediated inhibition (Doyon et al., 2011). Pre-treating slices with VU0240551 (n = 12 neurons) did not significantly alter the initial NMDAR mEPSCs: charge transfer (3.63 ± 0.31 pC, p = 0.25) was not different from slices with no VU0240551 pre-treatment (Figure 7A, left). Also, VU0240551-treated neurons did not display any time-dependent change in NMDAR charge transfer during recordings (Figure 7A, right).

As suppressing KCC2 function did not cause a potentiation of synaptic NMDAR responses per se, we asked whether this form of disinhibition may gate the potentiation of NMDAR mEPSCs by BDNF. In lamina I neurons from vehicle-treated slices of naive rats, bath-applying exogenous BDNF (100 ng/mL) after the start of whole-cell recording failed to produce potentiation of NMDAR mEPSCs and instead caused a small inhibition of synaptic NMDAR responses (n = 11 neurons, Figure 7B). However, in recordings from neurons in spinal slices that had been pre-treated with VU0240551, bath-applying BDNF (100 ng/mL) during the recording significantly increased NMDAR charge transfer (n = 5 neurons, p = 0.0072, Figure 7B).

In biochemical experiments, we found that BDNF pre-treatment reduced the level of KCC2 in the SDH (n = 8 slices,

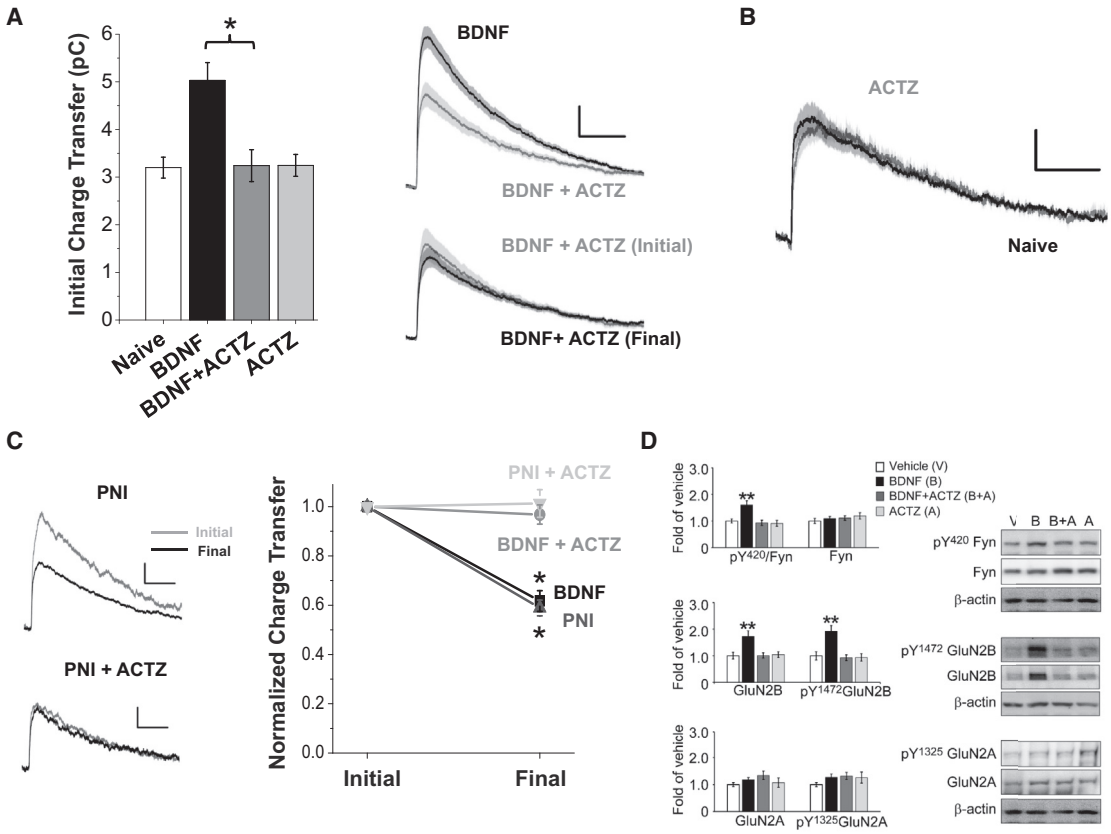

Figure 6. The Potentiation of NMDAR mEPSCs by BDNF/PNI Requires Disinhibition

(A) Left: plot of initial NMDAR charge transfer for slices pre-treated with saline (white), BDNF (black), BDNF and 10 μM acetazolamide (gray), or acetazolamide alone (light gray). Right top: average initial mEPSCs from naive slices pre-treated with BDNF (black) or with BDNF and 10 μM acetazolamide (gray). Right bottom: average mEPSCs for slices pre-treated with BDNF and 10 μM acetazolamide, during initial (gray) and final (black) recording periods.

(B) Initial average mEPSCs for slices pre-treated with 10 μM acetazolamide (n = 7) compared to saline pre-treated slices (n = 20).

(C) Left: representative mEPSC traces during initial (gray) and final (black) recording periods from lamina I neurons of the same PNI rat whereby one slice was pre-treated with control solution (top) and a separate slice was pre-treated with 10 μM acetazolamide for 72 min (bottom). Right: plot of normalized charge transfer values during initial and final recording periods. *p < 0.05 compared to initial charge transfer value for a given treatment. Scale bars, 100 ms (x axes); 5 pA (y axes).

(D) Western blots from synaptic fraction of SDH treated with either saline, BDNF, BDNF and acetazolamide, or acetazolamide alone. Statistical significance (*p < 0.05, n = 8 for all treatments) was determined using one-way ANOVA with Tukey's post hoc test.

All current traces and plots are represented as means ± SEM.

p = 0.042/0.0034, Figure 7C, top/bottom; Data S1) but not in the deep dorsal horn and ventral horn (Figure S4). Moreover, this reduction was not abolished by pre-treatment of BDNF with acetazolamide (n = 8 slice, p = 0.047, Figure 7C, top) nor TAT-Fyn39-57 (n = 8 slices, p = 0.00020, Figure 7C, bottom). As acetazolamide and TAT-Fyn39-57 did block the phosphorylation and potentiation of GluN2B NMDARs by BDNF, this finding further supports that KCC2 downregulation alone is not sufficient to induce potentiation of NMDARs. Thus, we conclude that not only does BDNF suppress KCC2-dependent inhibition but that the resultant disinhibition permits the action of this neurotrophin to potentiate synaptic GluN2B NMDARs via Fyn activation in lamina I neurons.

KCC2 level is regulated by several mechanisms following induction of neuronal activity (Chamma et al., 2013; Lee et al., 2011). To investigate whether calpain-mediated cleavage may be responsible for the loss of KCC2 upon BDNF treatment, we measured levels of fodrin—a well-characterized calpain substrate (Siman et al., 1984)—as a readout for calpain activity. We found no changes in full-length (250 kDa) or calpain-cleaved (150/145 kDa) fragments of fodrin after BDNF treatment in SDH synaptosomes (Figure S5A) or SDH homogenates (Figure S5B), suggesting calpain was not activated by BDNF under these conditions.

Raising Intracellular Ca^{2+} Permits BDNF-Induced Potentiation of NMDAR mEPSCs

We next investigated how disinhibition may gate subsequent potentiation of synaptic NMDARs by BDNF. The acetazolamide experiments suggest that a rise in intracellular Cl^- does not permit the potentiation of synaptic NMDARs by the TrkB/Fyn pathway. As disinhibition also induces an increase in intracellular $[Ca^{2+}]$ ($[Ca^{2+}]_i$) in spinal neurons (Darbon et al., 2002), it is possible that a rise in $[Ca^{2+}]_i$ gates the effect of BDNF on

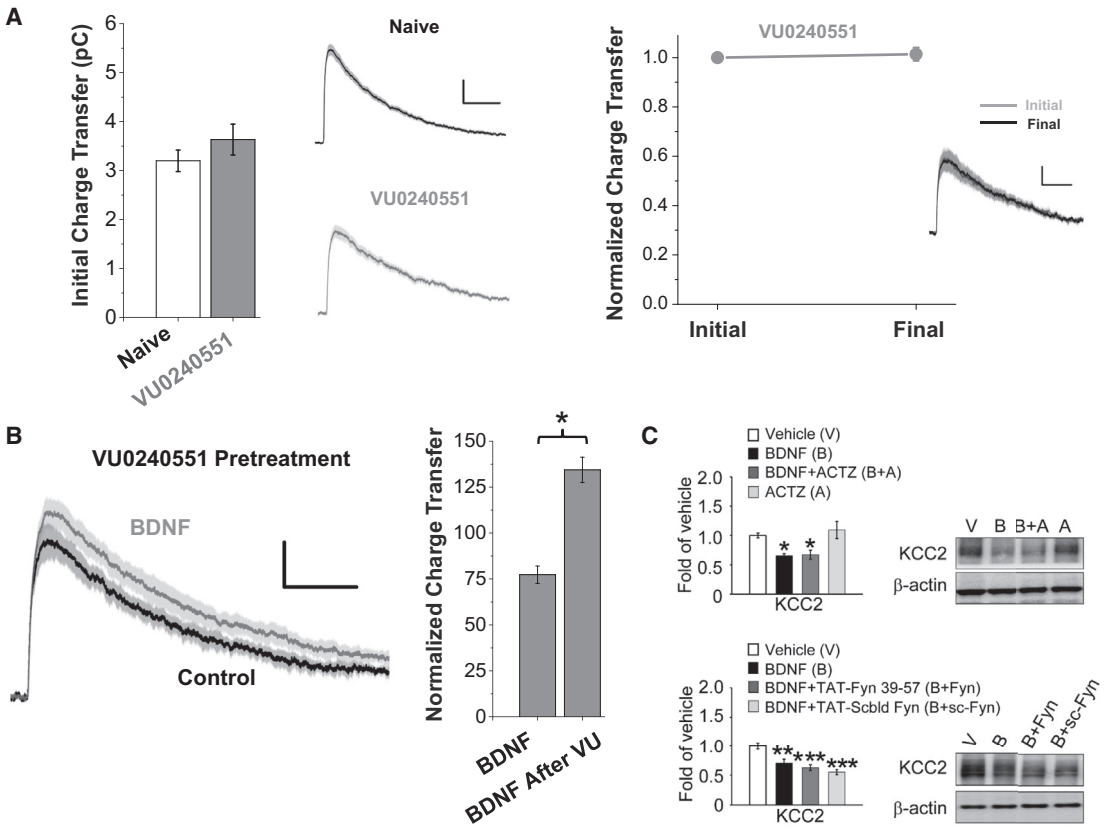

Figure 7. Downregulation of KCC2 Activity Gates Potentiation of NMDAR mEPSCs by Exogenous BDNF

(A) Average initial mEPSC traces (middle) and associated NMDAR charge transfer values (left) in control-treated slices (white) or slices pre-treated with 50 μM VU0240551 for 80 ± 3 min (gray, n = 12). Right: average mEPSC traces (inset) and normalized charge transfer values for slices pre-treated with VU0240551 during initial and final recording periods.

(B) Left: average mEPSC traces from slices pre-treated VU0240551 for 60+ min (n = 5). Following a control period of recording (black trace), 100 ng/mL BDNF was acutely perfused during recording for 10+ min (gray trace). Right: NMDAR charge transfer during acute administration of BDNF normalized to a control recording period for untreated (left bar) and VU0240551 pre-treated (right bar) slices. *p < 0.05. Scale bars, 100 ms (x axes); 5 pA (y axes).

(C) Synaptic fraction from SDH treated with the indicated agents for 70 min. KCC2 protein levels were normalized to beta-actin as a loading control (left). Statistical significance (*p < 0.05, n = 8) was determined one-way ANOVA with Tukey's post hoc test.

All current traces and plots are represented as means ± SEM.

NMDARs at lamina I synapses. Hence, we studied NMDAR mEPSCs in lamina I neurons of naive rats under conditions that permit, or prevent, an increase in $[Ca^{2+}]_i$. To facilitate increasing $[Ca^{2+}]_i$ we used an extracellular recording solution lacking Cd^{2+} and Mg^{2+} to permit and enhance calcium influx through voltage-gated calcium channels and NMDARs, respectively. Moreover, we reduced intracellular Ca^{2+} buffering by using 100 μM EGTA in the intracellular pipette solution. Under these recording conditions, NMDAR mEPSCs at −40 mV remained constant during 20 min of whole-cell recording: the charge transfer of inward NMDAR mEPSCs was not significantly different between the 10–15 min recording period (Q = −0.45 ± 0.11, n = 6) and the 15–20 min recording period (Q = −0.44 ± 0.11 pC, n = 6, p = 0.75; Figure S6). However, we found under these recording conditions that administrating exogenous BDNF induced an increase in NMDAR mEPSCs (Figure S7): average NMDAR charge transfer significantly increased from −0.45 ± 0.11 pC during baseline recording to −0.83 ± 0.16 pC during administration of BDNF (n = 6 neurons, p = 0.0021, Figure S7B, left). This BDNF-induced increase in NMDAR charge transfer was not observed in neurons where we greatly increased intracellular Ca^{2+} buffering by replacing EGTA (100 μM) with the more rapid buffer BAPTA at the higher concentration of 10 mM (Figure S7B, right; baseline Q = −0.45 ± 0.10 pC, BDNF Q = −0.51 ± 0.10 pC, n = 5). Thus, an increase in $[Ca^{2+}]_i$ within the lamina I neuron recorded is permissive for the subsequent potentiation of synaptic NMDARs by BDNF.

DISCUSSION

Given the importance of lamina I neurons to the integration and output of spinal nociceptive signals (Braz et al., 2014; Prescott et al., 2014), we investigated whether glutamatergic responses at lamina I synapses are altered in a model of neuropathic pain. We found that unitary synaptic NMDAR currents in lamina I spinal neurons are potentiated following traumatic peripheral

nerve injury. The AMPAR component of the mEPSCs, by contrast, was unchanged by nerve injury indicating that the quantal release of glutamate onto lamina I neurons is not altered by PNI, consistent with previous reports (Chen et al., 2014a; Li et al., 2016). Rather, our findings indicate that the increase in the NMDAR component of the mEPSCs in the nerve-injured state is mediated post-synaptically by enhancement of NMDARs in the lamina I neurons themselves. The most parsimonious signaling cascade suggested by our results is that activation of TrkB by its cognate ligand BDNF leads to activation of Fyn kinase and potentiation of GluN2B-containing synaptic NMDARs. Unexpectedly, the potentiation of NMDARs by the BDNF-TrkB-Fyn signaling pathway requires prior and sustained KCC2-dependent disinhibition, as we found that blocking disinhibition with acetazolamide abolished the enhancement of lamina I NMDARs by exogenously administered BDNF or nerve injury. Thus, taking our evidence together suggests that within individual lamina I neurons, BDNF-mediated disinhibition leads to a post-synaptic rise in $[Ca^{2+}]_i$ that gates potentiation of synaptic GluN2B NMDARs, by the TrkB-Fyn signaling pathway, in a feed-forward cycle that is activated by nerve injury.

Our findings indicate that ongoing release of BDNF and continuous activation of TrkB-Fyn signaling is required to maintain the basal potentiation of NMDAR responses at lamina I synapses. Specifically, we found that NMDAR mEPSCs in lamina I neurons from animals with PNI were robustly potentiated even several hours after sectioning—potentiation that was reversed by acute blockade of TrkB, Fyn, or disinhibition. From these findings, we conclude that following nerve injury, a BDNF-mediated signaling cascade that includes spinal disinhibition and activation of TrkB and Fyn within individual lamina I neurons is being continuously activated and is required for basal NMDAR potentiation. Thus, the potentiation of NMDARs at lamina I synapses is not an event induced by PNI and maintained independently, like activity-induced long-term potentiation. A form of long-term potentiation has been shown at lamina I synapses following peripheral inflammation (Ikeda et al., 2006), and it is possible that the basal potentiation of synaptic NMDARs observed here can lead to a facilitation of synaptic AMPAR responses following a train of afferent firing. However, unlike canonical long term potentiation, the basal potentiation of synaptic NMDARs in lamina I neurons is maintained by ongoing signaling. This conclusion is consistent with the behavioral sensitization in PNI models that is reversed by interfering with specific elements of the signaling cascade. For example, PNI-induced behavioral sensitization is reversed by BDNF-TrkB blockers (Coull et al., 2005; Wang et al., 2009), NMDAR antagonists (Bourinet et al., 2014), SFK inhibitors (Peng et al., 2010), and blockers of KCC2-dependent spinal disinhibition (Asiedu et al., 2010; Gagnon et al., 2013; Li et al., 2016).

Potentiation of NMDAR by SFKs is known to depend upon tyrosine residues on the GluN2 subunits (Salter and Kalia, 2004) with different SFKs preferentially potentiating NMDARs comprised of different GluN2 subunits (Salter et al., 2009). The GluN2 subunit dependency has been worked out most extensively with NMDAR responses in hippocampal CA1 neurons. In CA1 neurons, Fyn selectively phosphorylates and enhances the activity of GluN2B-containing NMDARs, while Src phosphorylates and enhances GluN2A-containing receptors (Yang et al., 2012). In spinal lamina I neurons, NMDAR mEPSCs are dominated by GluN2B subunits with little contribution from GluN2A-containing receptors (Hildebrand et al., 2014). This GluN2B dominance is consistent with our findings showing that the potentiation of NMDAR mEPSCs after PNI is dependent on Fyn, but not Src activity. Indeed, we show that Fyn directly potentiates GluN2B NMDAR responses at lamina I synapses and that BDNF mediates an increase in the activated/phosphorylated forms of Fyn and GluN2B proteins selectively at SDH synapses. Thus, we conclude that GluN2B-containing NMDARs in lamina I neurons are selectively enhanced by Fyn kinase, activated downstream of TrkB. Conversely, although phosphorylation of NMDARs by Src has been implicated in pain hypersensitivity (Liu et al., 2008), GluN2A-containing NMDARs contribute little to NMDAR mEPSCs in lamina I neurons (Hildebrand et al., 2014). We observe here that the Src inhibitor peptide had no effect on the potentiation of NMDAR mEPSCs after PNI and that BDNF did not alter GluN2A expression or phosphorylation at SDH synapses. We therefore conclude that the regulation of NMDARs by Src that is linked to pathological pain occurs at a locus in the pain transmission pathway other than in lamina I spinal neurons. Potential sites where Src-dependent potentiation of NMDARs may mediate pain hypersensitivity include presynaptic afferents (Chen et al., 2014b) and lamina II neurons (Wang et al., 2016).

The reversal of PNI-induced potentiation of NMDAR mEPSCs by acetazolamide implies that spinal disinhibition is required for the potentiation of NMDAR responses at lamina I synapses. One possible mechanism is that the increase in Cl^- that is produced by decreased KCC2 activity in individual lamina I neurons (Coull et al., 2003) gates the potentiation of NMDARs by Fyn. However, acetazolamide should not alter intracellular Cl^- concentration, as it blocks intracellular HCO_3^- production to reverse disinhibition (Staley et al., 1995). We also found that treating naive slices with the KCC2 antagonist, VU0240551, had no effect on NMDAR mEPSCs in lamina I neurons. Thus, an increase in intracellular Cl^- is not sufficient for the potentiation of NMDARs at lamina I synapses. One potential player in this process is the protein tyrosine phosphatase $STEP_{61}$. $STEP_{61}$ dephosphorylates and inactivates Fyn, and not Src, and dephosphorylates GluN2B, leading to internalization of GluN1/GluN2B receptor complexes (Azkona et al., 2016; Xu et al., 2015). Disinhibition may thereby drive a downregulation of $STEP_{61}$ to gate NMDAR potentiation by BDNF. As neither the disinhibition pathway alone nor the BDNF-TrkB signaling pathway alone is sufficient to cause potentiation of synaptic NMDAR currents, these processes appear to require coincident activation to cause potentiation of NMDARs. Together, the data indicate that we have discovered a form of molecular coincidence detection in lamina I neurons that requires ongoing inputs—BDNF-TrkB signaling and spinal disinhibition—to mediate the potentiation of synaptic excitation.

The relationship between disinhibition and NMDAR potentiation is a feed-forward mechanism for accelerating enhancement of overall excitability of lamina I neurons. The relationship may also be reciprocal. It has recently been shown that NMDAR activity and an increase in $[Ca^{2+}]_i$ are required for the downregulation of KCC2 in the brain and spinal cord (Chamma et al., 2013;

Lee et al., 2011; Zhou et al., 2012), implying a vicious cycle within lamina I neurons whereby loss of inhibition gates an increase in excitation and vice versa. The potential therapeutic implications of such a cycle might be that blocking disinhibition may secondarily relieve the permissive effect that is needed for NMDAR potentiation, while blocking NMDAR activity may relieve the drive to downregulate KCC2. In support, blockade of the individual molecular players in this pathway has been shown to reverse nerve-injury induced hypersensitivity in vivo, including BDNF (Coull et al., 2005), KCC2 downregulation (Li et al., 2016), disinhibition (Coull et al., 2003; Lee and Prescott, 2015), Fyn activation (Abe et al., 2005; Katsura et al., 2006; Liu et al., 2014), interactions between Fyn and pY1472-GluN2B (Matsumura et al., 2010), and GluN2B function (Kim et al., 2012). Thus, our results provide a biologically plausible model of molecular coupling within lamina I neurons that may explain how multiple signaling pathways might each be necessary to sustain nerve-injury induced hypersensitivity.

We speculate that our findings have implications beyond understanding nerve-injury induced hypersensitivity, as BDNF has been implicated in other types of pain hypersensitivity. In inflammatory hypersensitivity, BDNF appears to be released from nociceptive primary afferents, and knocking down nociceptor BDNF selectively attenuates behavioral hypersensitivity induced by peripheral inflammation (Mannion et al., 1999; Zhao et al., 2006) and burst stimulation of afferents drives BDNF release (Lever et al., 2001). In morphine-induced hyperalgesia, BDNF released from activated spinal microglia mediates a disinhibition in lamina I neurons that drives sensitization (Ferrini et al., 2013). Thus, our present findings raise the possibility that BDNF-mediated disinhibition may drive NMDAR potentiation in a number of hypersensitivity states in the spinal cord. Finally, both BDNF-evoked disinhibition and potentiation of synaptic NMDARs can occur at synapses throughout the brain, and coupling between these pathways could underlie neuronal hyperexcitability in disorders ranging from addiction to traumatic brain injury to epilepsy (Ferrini and De Koninck, 2013; Kalia et al., 2008; Semaan et al., 2015; Shulga et al., 2008; Vargas-Perez et al., 2014). We therefore propose that our model of coincident detection between facilitation of NMDAR-mediated excitation and loss of KCC2-dependent inhibition may be broadly relevant to synaptic signaling throughout the CNS.

EXPERIMENTAL PROCEDURES

Animals

All experiments involving rats and their care were performed in accordance with the recommendations of the Canadian Council on Animal Care and were according to the animal care regulations and policies of the Hospital for Sick Children, Toronto. We performed all experiments on male adult (350–450 g) Sprague Dawley (SD) rats, except for the experiments in Figure 3A, which utilized juvenile (P20–P22) SD rats.

Peripheral Nerve Injury and Behavioral Testing

As previously described (Mosconi and Kruger, 1996; Pitcher et al., 1999), we used a PNI model of neuropathic pain to study pathological pain signaling. Under isoflurane anesthesia, we implanted a 2-mm long polyethylene cuff around the sciatic nerve of adult SD rats. Ten to 17 days after surgery, animals were tested for behavioral hypersensitivity compared to baseline by measuring mechanical paw withdrawal threshold with von Frey filaments. Animals used for spinal slice electrophysiology typically had a reduction in paw withdrawal threshold from 15 g to 4 g, which was restricted to the ipsilateral paw.

Spinal Cord Isolation

We anaesthetized male SD rats through intraperitoneal (i.p.) injection of 3 g/kg urethane (Sigma). As previously described (Hildebrand et al., 2014), we rapidly dissected out the lumbar spinal cord and immediately placed the cord in an ice-cold, oxygenated protective modified artificial cerebrospinal fluid (pACSF) solution. Parasagittal spinal slices (300 μm) were cut from an L3–L6 section of lumbar spinal cord.

Electrophysiological Recordings on Lamina I Spinal Cord Neurons

We visualized cells using infrared differential interference contrast (IR-DIC) optics and neurons from lamina I were selected based upon their location dorsal to the substantia gelatinosa layer, within 50 μm of the white matter (Hildebrand et al., 2014). Although this selection criteria enriches for a population of mainly lamina I neurons, we cannot formally exclude the possibility that a smaller fraction of recorded neurons were in lamina II.

The extracellular recording solution consisted of an artificial cerebrospinal fluid (ACSF) solution containing (in mM): 125 NaCl, 20 D-glucose, 26 $NaHCO_3$, 3 KCl, 1.25 NaH_2PO_4, 2 $CaCl_2$, and 1 $MgCl_2$ as well as 500 nM TTX, 10 μM Cd^{2+}, 10 μM strychnine and 10 μM bicuculline to block voltage-gated Na^+ channel, voltage-gated Ca^{2+} channel, glycinergic and GABAergic currents, respectively. We pulled patch-clamp pipettes with resistances of 4–8 MΩ. The internal patch pipette solution contained (in mM): 105 Cs-gluconate, 17.5 CsCl, 10 BAPTA, 10 HEPES, 5 QX-314, 2 MgATP, 0.5 Na_2GTP (pH = 7.25, 295 mOsm), except in a subset of experiments where 10 BAPTA was replaced with 0.1 EGTA (Figure S7).

Neurons typically had access resistances below 20 MΩ and leakage currents >−100 pA at a holding potential (V_h) of −70 mV. As previously described (Hildebrand et al., 2014), we generated averaged mEPSCs for time intervals ranging between 5 and 10 min, typically with 30 to 50 events per averaged trace. For recordings of NMDAR-mEPSCs at +60 mV, we broke through to the whole-cell configuration at −60 mV and gradually adjusted the holding potential to +60 mV. Thus, analysis of "initial" NMDAR-mEPSC currents was based on averages from ~5–15 min after whole-cell configuration. We selected for mEPSCs containing a NMDAR component at +60 mV by excluding mEPSCs that exhibited complete decay within 100 ms. For experiments with conditions that promoted a rise in intracellular Ca^{2+} (Figures S6 and S7), recordings were done at a holding potential of −40 mV, on neurons with a mEPSC frequency >1 Hz.

Compounds and Perfusion

For electrophysiology experiments, D-AP5, bicuculline methochloride, K252a, Ro25-6981, TCN-201. and VU 0240551 were from Tocris Bioscience. TTX was from Alomone labs. Recombinant BDNF protein was from Abcam, while TrkB-Fc and TrkB-IgG were from R&D Systems. Ionomycin, PP2 and SU6656 were from Calbiochem. The Src40-58 and Fyn39-57 inhibitor peptides as well as their TAT-linked versions (Liu et al., 2008; Yang et al., 2012) were synthesized by GenScript. Unless otherwise indicated, all other compounds were ordered from Sigma-Aldrich. We applied 50 ng/mL BDNF in slice pre-treatment experiments, where prolonged treatment would allow for permeation of BDNF throughout the slice. A higher concentration of BDNF (100 ng/mL) was used for acute perfusion to ensure that sufficient levels of BDNF reached the neuron under study during the shorter time course of the recordings.

Isolation of Synaptic Fractions and Biochemical Analyses

For biochemical studies, the lumbar spinal cord was sectioned horizontally with a vibratome into an approximately 300 μm thick horizontal SDH section and a second section containing the remainder of the spinal cord. Isolation of synaptic fractions was performed as previously described (Xu et al., 2009). Briefly, tissues were lysed in Dounce tissue grinders (Wheaton) in 1 mL ice-cold TEVP buffer supplemented with complete protease inhibitor cocktail (Roche). Aliquots of lysates were saved for further analyses as total homogenates. The rest of lysates went through two spins (10 min at 1,000 × *g* and 15 min at 12,000 × *g*) to obtain synaptic fractions. Samples (30 μg) were loaded on 8% SDS-PAGE and transferred to nitrocellulose

membrane (Bio-Rad). Membranes were blocked in 5% BSA in TBS + 1% Tween-20 (TBS-T) and incubated with primary antibodies overnight (anti-pY^{416} Src family [1:1,000] and anti-pY^{527} Src family [1:1,000] from Upstate; anti-Fyn [1:2,000], anti-Src [1:2,000], anti-KCC2 [1:2,000] and anti-actin [1:5,000] from Santa Cruz; anti-pY^{1472} GluN2B [1:1,000] and anti-pY^{1325} GluN2A [1:1,000] from PhosphoSolutions; anti-GluN2B [1:2,000] and anti-GluN2A [1:2,000] from Millipore; anti-fodrin [1:5,000] from Enzo Life Sciences) in 5% BSA+TBS-T. Membranes were washed three times with TBS-T and then incubated with horseradish peroxidase (HRP)-coupled secondary antibodies (anti-mouse or anti-rabbit, Pierce, 1:5,000) for 2 hr at room temperature. Membranes were developed using Chemiluminescent Substrate kit (Pierce) and visualized by a G:BOX with the GeneSnap software (Syngene). All densitometric bands were quantified using ImageJ (NIH).

Data Analysis

We used Microcal Origin 8.5 (Northampton) and Clampfit10 (Molecular Devices) for data analysis. All data are given as means ± SEM. We performed statistical comparisons of data using both Student's paired and unpaired t tests as well as one-way ANOVAs followed by a Tukey's test for means comparisons. We considered $p < 0.05$ to be statistically significant.

SUPPLEMENTAL INFORMATION

Supplemental Information includes seven figures, three tables, and one data file and can be found with this article online at http://dx.doi.org/10.1016/j.celrep.2016.11.024.

AUTHOR CONTRIBUTIONS

Experiments were designed by M.E.H., S.B., P.J.L. and M.W.S. M.E.H., J.X., A.D., Y.L., and A.S.S. conducted the experiments and analyzed the data. M.E.H. and M.W.S. wrote the majority of the manuscript, with contributions and edits from J.X., A.S.S., S.B., and P.J.L.

ACKNOWLEDGMENTS

We dedicate this paper to our dear friend Dr. John F. MacDonald, who was taken from us much too soon. This study was supported by a grant from CIHR to M.W.S. (MT-12682) and grants from NSERC (Discovery Grant), IASP (Early Career Research Grant), the Canadian Pain Society, and Pfizer Canada (Early Career Investigator Pain Research Grant) to M.E.H. M.W.S. holds the Northbridge Chair in Paediatric Research. M.E.H. was initially supported by a postdoctoral fellowship from CIHR and a Pain Scientist Award from the University of Toronto Centre for the Study of Pain.

Received: December 10, 2014
Revised: October 14, 2016
Accepted: November 3, 2016
Published: December 6, 2016

REFERENCES

Abe, T., Matsumura, S., Katano, T., Mabuchi, T., Takagi, K., Xu, L., Yamamoto, A., Hattori, K., Yagi, T., Watanabe, M., et al. (2005). Fyn kinase-mediated phosphorylation of NMDA receptor NR2B subunit at Tyr1472 is essential for maintenance of neuropathic pain. Eur. J. Neurosci. *22*, 1445–1454.

Asiedu, M., Ossipov, M.H., Kaila, K., and Price, T.J. (2010). Acetazolamide and midazolam act synergistically to inhibit neuropathic pain. Pain *148*, 302–308.

Azkona, G., Saavedra, A., Aira, Z., Aluja, D., Xifró, X., Baguley, T., Alberch, J., Ellman, J.A., Lombroso, P.J., Azkue, J.J., and Pérez-Navarro, E. (2016). Striatal-enriched protein tyrosine phosphatase modulates nociception: evidence from genetic deletion and pharmacological inhibition. Pain *157*, 377–386.

Beggs, S., and Salter, M.W. (2013). The known knowns of microglia-neuronal signalling in neuropathic pain. Neurosci. Lett. *557*, 37–42.

Beggs, S., Trang, T., and Salter, M.W. (2012). P2X4R+ microglia drive neuropathic pain. Nat. Neurosci. *15*, 1068–1073.

Bourinet, E., Altier, C., Hildebrand, M.E., Trang, T., Salter, M.W., and Zamponi, G.W. (2014). Calcium-permeable ion channels in pain signaling. Physiol. Rev. *94*, 81–140.

Braz, J., Solorzano, C., Wang, X., and Basbaum, A.I. (2014). Transmitting pain and itch messages: a contemporary view of the spinal cord circuits that generate gate control. Neuron *82*, 522–536.

Chamma, I., Heubl, M., Chevy, Q., Renner, M., Moutkine, I., Eugène, E., Poncer, J.C., and Lévi, S. (2013). Activity-dependent regulation of the K/Cl transporter KCC2 membrane diffusion, clustering, and function in hippocampal neurons. J. Neurosci. *33*, 15488–15503.

Chen, S.R., Hu, Y.M., Chen, H., and Pan, H.L. (2014a). Calcineurin inhibitor induces pain hypersensitivity by potentiating pre- and postsynaptic NMDA receptor activity in spinal cords. J. Physiol. *592*, 215–227.

Chen, W., Walwyn, W., Ennes, H.S., Kim, H., McRoberts, J.A., and Marvizón, J.C. (2014b). BDNF released during neuropathic pain potentiates NMDA receptors in primary afferent terminals. Eur. J. Neurosci. *39*, 1439–1454.

Coull, J.A., Boudreau, D., Bachand, K., Prescott, S.A., Nault, F., Sík, A., De Koninck, P., and De Koninck, Y. (2003). Trans-synaptic shift in anion gradient in spinal lamina I neurons as a mechanism of neuropathic pain. Nature *424*, 938–942.

Coull, J.A., Beggs, S., Boudreau, D., Boivin, D., Tsuda, M., Inoue, K., Gravel, C., Salter, M.W., and De Koninck, Y. (2005). BDNF from microglia causes the shift in neuronal anion gradient underlying neuropathic pain. Nature *438*, 1017–1021.

Darbon, P., Pignier, C., Niggli, E., and Streit, J. (2002). Involvement of calcium in rhythmic activity induced by disinhibition in cultured spinal cord networks. J. Neurophysiol. *88*, 1461–1468.

Delpire, E., Days, E., Lewis, L.M., Mi, D., Kim, K., Lindsley, C.W., and Weaver, C.D. (2009). Small-molecule screen identifies inhibitors of the neuronal K-Cl cotransporter KCC2. Proc. Natl. Acad. Sci. USA *106*, 5383–5388.

Doyon, N., Prescott, S.A., Castonguay, A., Godin, A.G., Kröger, H., and De Koninck, Y. (2011). Efficacy of synaptic inhibition depends on multiple, dynamically interacting mechanisms implicated in chloride homeostasis. PLoS Comput. Biol. *7*, e1002149.

Ferrini, F., and De Koninck, Y. (2013). Microglia control neuronal network excitability via BDNF signalling. Neural Plast. *2013*, 429815.

Ferrini, F., Trang, T., Mattioli, T.A., Laffray, S., Del'Guidice, T., Lorenzo, L.E., Castonguay, A., Doyon, N., Zhang, W., Godin, A.G., et al. (2013). Morphine hyperalgesia gated through microglia-mediated disruption of neuronal Cl^- homeostasis. Nat. Neurosci. *16*, 183–192.

Gagnon, M., Bergeron, M.J., Lavertu, G., Castonguay, A., Tripathy, S., Bonin, R.P., Perez-Sanchez, J., Boudreau, D., Wang, B., Dumas, L., et al. (2013). Chloride extrusion enhancers as novel therapeutics for neurological diseases. Nat. Med. *19*, 1524–1528.

Hildebrand, M.E., Pitcher, G.M., Harding, E.K., Li, H., Beggs, S., and Salter, M.W. (2014). GluN2B and GluN2D NMDARs dominate synaptic responses in the adult spinal cord. Sci. Rep. *4*, 4094.

Ikeda, H., Stark, J., Fischer, H., Wagner, M., Drdla, R., Jäger, T., and Sandkühler, J. (2006). Synaptic amplifier of inflammatory pain in the spinal dorsal horn. Science *312*, 1659–1662.

Ingley, E. (2008). Src family kinases: regulation of their activities, levels and identification of new pathways. Biochim. Biophys. Acta *1784*, 56–65.

Kaila, K., Price, T.J., Payne, J.A., Puskarjov, M., and Voipio, J. (2014). Cation-chloride cotransporters in neuronal development, plasticity and disease. Nat. Rev. Neurosci. *15*, 637–654.

Kalia, L.V., Kalia, S.K., and Salter, M.W. (2008). NMDA receptors in clinical neurology: excitatory times ahead. Lancet Neurol. *7*, 742–755.

Katsura, H., Obata, K., Mizushima, T., Sakurai, J., Kobayashi, K., Yamanaka, H., Dai, Y., Fukuoka, T., Sakagami, M., and Noguchi, K. (2006). Activation of Src-family kinases in spinal microglia contributes to mechanical hypersensitivity after nerve injury. J. Neurosci. *26*, 8680–8690.

Keller, A.F., Beggs, S., Salter, M.W., and De Koninck, Y. (2007). Transformation of the output of spinal lamina I neurons after nerve injury and microglia stimulation underlying neuropathic pain. Mol. Pain *3*, 27.

Kim, Y., Cho, H.Y., Ahn, Y.J., Kim, J., and Yoon, Y.W. (2012). Effect of NMDA NR2B antagonist on neuropathic pain in two spinal cord injury models. Pain *153*, 1022–1029.

Lee, K.Y., and Prescott, S.A. (2015). Chloride dysregulation and inhibitory receptor blockade yield equivalent disinhibition of spinal neurons yet are differentially reversed by carbonic anhydrase blockade. Pain *156*, 2431–2437.

Lee, H.H., Deeb, T.Z., Walker, J.A., Davies, P.A., and Moss, S.J. (2011). NMDA receptor activity downregulates KCC2 resulting in depolarizing GABAA receptor-mediated currents. Nat. Neurosci. *14*, 736–743.

Lever, I.J., Bradbury, E.J., Cunningham, J.R., Adelson, D.W., Jones, M.G., McMahon, S.B., Marvizón, J.C., and Malcangio, M. (2001). Brain-derived neurotrophic factor is released in the dorsal horn by distinctive patterns of afferent fiber stimulation. J. Neurosci. *21*, 4469–4477.

Li, L., Chen, S.R., Chen, H., Wen, L., Hittelman, W.N., Xie, J.D., and Pan, H.L. (2016). Chloride homeostasis critically regulates synaptic NMDA receptor activity in neuropathic pain. Cell Rep. *15*, 1376–1383.

Liu, X.J., Gingrich, J.R., Vargas-Caballero, M., Dong, Y.N., Sengar, A., Beggs, S., Wang, S.H., Ding, H.K., Frankland, P.W., and Salter, M.W. (2008). Treatment of inflammatory and neuropathic pain by uncoupling Src from the NMDA receptor complex. Nat. Med. *14*, 1325–1332.

Liu, Y.N., Yang, X., Suo, Z.W., Xu, Y.M., and Hu, X.D. (2014). Fyn kinase-regulated NMDA receptor- and AMPA receptor-dependent pain sensitization in spinal dorsal horn of mice. Eur. J. Pain *18*, 1120–1128.

Mannion, R.J., Costigan, M., Decosterd, I., Amaya, F., Ma, Q.P., Holstege, J.C., Ji, R.R., Acheson, A., Lindsay, R.M., Wilkinson, G.A., and Woolf, C.J. (1999). Neurotrophins: peripherally and centrally acting modulators of tactile stimulus-induced inflammatory pain hypersensitivity. Proc. Natl. Acad. Sci. USA *96*, 9385–9390.

Matsumura, S., Kunori, S., Mabuchi, T., Katano, T., Nakazawa, T., Abe, T., Watanabe, M., Yamamoto, T., Okuda-Ashitaka, E., and Ito, S. (2010). Impairment of CaMKII activation and attenuation of neuropathic pain in mice lacking NR2B phosphorylated at Tyr1472. Eur. J. Neurosci. *32*, 798–810.

Mosconi, T., and Kruger, L. (1996). Fixed-diameter polyethylene cuffs applied to the rat sciatic nerve induce a painful neuropathy: ultrastructural morphometric analysis of axonal alterations. Pain *64*, 37–57.

Ninkina, N., Grashchuck, M., Buchman, V.L., and Davies, A.M. (1997). TrkB variants with deletions in the leucine-rich motifs of the extracellular domain. J. Biol. Chem. *272*, 13019–13025.

Peng, H.Y., Chen, G.D., Lai, C.H., Tung, K.C., Chang, J.L., and Lin, T.B. (2010). Endogenous ephrinB2 mediates colon-urethra cross-organ sensitization via Src kinase-dependent tyrosine phosphorylation of NR2B. Am. J. Physiol. Renal Physiol. *298*, F109–F117.

Pitcher, G.M., Ritchie, J., and Henry, J.L. (1999). Paw withdrawal threshold in the von Frey hair test is influenced by the surface on which the rat stands. J. Neurosci. Methods *87*, 185–193.

Prescott, S.A., Ma, Q., and De Koninck, Y. (2014). Normal and abnormal coding of somatosensory stimuli causing pain. Nat. Neurosci. *17*, 183–191.

Price, T.J., Cervero, F., Gold, M.S., Hammond, D.L., and Prescott, S.A. (2009). Chloride regulation in the pain pathway. Brain Res. Brain Res. Rev. *60*, 149–170.

Salter, M.W., and Kalia, L.V. (2004). Src kinases: a hub for NMDA receptor regulation. Nat. Rev. Neurosci. *5*, 317–328.

Salter, M.W., Dong, Y., Kalia, L.V., Liu, X.J., and Pitcher, G. (2009). Regulation of NMDA receptors by kinases and phosphatases. In Biology of the NMDA Receptor, A.M. Van Dongen, ed. (CRC Press/Taylor & Francis).

Semaan, S., Wu, J., Gan, Y., Jin, Y., Li, G.H., Kerrigan, J.F., Chang, Y.C., and Huang, Y. (2015). Hyperactivation of BDNF-TrkB signaling cascades in human hypothalamic hamartoma (HH): a potential mechanism contributing to epileptogenesis. CNS Neurosci. Ther. *21*, 164–172.

Shulga, A., Thomas-Crusells, J., Sigl, T., Blaesse, A., Mestres, P., Meyer, M., Yan, Q., Kaila, K., Saarma, M., Rivera, C., and Giehl, K.M. (2008). Posttraumatic GABA(A)-mediated [Ca2+]i increase is essential for the induction of brain-derived neurotrophic factor-dependent survival of mature central neurons. J. Neurosci. *28*, 6996–7005.

Siman, R., Baudry, M., and Lynch, G. (1984). Brain fodrin: substrate for calpain I, an endogenous calcium-activated protease. Proc. Natl. Acad. Sci. USA *81*, 3572–3576.

Staley, K.J., Soldo, B.L., and Proctor, W.R. (1995). Ionic mechanisms of neuronal excitation by inhibitory GABAA receptors. Science *269*, 977–981.

Tapley, P., Lamballe, F., and Barbacid, M. (1992). K252a is a selective inhibitor of the tyrosine protein kinase activity of the trk family of oncogenes and neurotrophin receptors. Oncogene *7*, 371–381.

Todd, A.J. (2010). Neuronal circuitry for pain processing in the dorsal horn. Nat. Rev. Neurosci. *11*, 823–836.

Vargas-Perez, H., Bahi, A., Bufalino, M.R., Ting-A-Kee, R., Maal-Bared, G., Lam, J., Fahmy, A., Clarke, L., Blanchard, J.K., Larsen, B.R., et al. (2014). BDNF signaling in the VTA links the drug-dependent state to drug withdrawal aversions. J. Neurosci. *34*, 7899–7909.

Wang, Y.T., and Salter, M.W. (1994). Regulation of NMDA receptors by tyrosine kinases and phosphatases. Nature *369*, 233–235.

Wang, X., Ratnam, J., Zou, B., England, P.M., and Basbaum, A.I. (2009). TrkB signaling is required for both the induction and maintenance of tissue and nerve injury-induced persistent pain. J. Neurosci. *29*, 5508–5515.

Wang, X.T., Zheng, R., Suo, Z.W., Liu, Y.N., Zhang, Z.Y., Ma, Z.A., Xue, Y., Xue, M., Yang, X., and Hu, X.D. (2016). Activity-dependent dephosphorylation of paxillin contributed to nociceptive plasticity in spinal cord dorsal horn. Pain *157*, 652–665.

Woolf, C.J., and Salter, M.W. (2000). Neuronal plasticity: increasing the gain in pain. Science *288*, 1765–1769.

Xu, J., Kurup, P., Zhang, Y., Goebel-Goody, S.M., Wu, P.H., Hawasli, A.H., Baum, M.L., Bibb, J.A., and Lombroso, P.J. (2009). Extrasynaptic NMDA receptors couple preferentially to excitotoxicity via calpain-mediated cleavage of STEP. J. Neurosci. *29*, 9330–9343.

Xu, J., Kurup, P., Foscue, E., and Lombroso, P.J. (2015). Striatal-enriched protein tyrosine phosphatase regulates the PTPα/Fyn signaling pathway. J. Neurochem. *134*, 629–641.

Yang, K., Trepanier, C., Sidhu, B., Xie, Y.F., Li, H., Lei, G., Salter, M.W., Orser, B.A., Nakazawa, T., Yamamoto, T., et al. (2012). Metaplasticity gated through differential regulation of GluN2A versus GluN2B receptors by Src family kinases. EMBO J. *31*, 805–816.

Zhao, J., Seereeram, A., Nassar, M.A., Levato, A., Pezet, S., Hathaway, G., Morenilla-Palao, C., Stirling, C., Fitzgerald, M., McMahon, S.B., et al.; London Pain Consortium (2006). Nociceptor-derived brain-derived neurotrophic factor regulates acute and inflammatory but not neuropathic pain. Mol. Cell. Neurosci. *31*, 539–548.

Zhou, H.Y., Chen, S.R., Byun, H.S., Chen, H., Li, L., Han, H.D., Lopez-Berestein, G., Sood, A.K., and Pan, H.L. (2012). N-methyl-D-aspartate receptor- and calpain-mediated proteolytic cleavage of K+-Cl- cotransporter-2 impairs spinal chloride homeostasis in neuropathic pain. J. Biol. Chem. *287*, 33853–33864.